

# Re-Os Dating of Polymetallic Ni-Mo-PGE-Au Mineralization in Lower Cambrian Black Shales of South China and Its Geologic Significance

JINGWEN MAO,

*Institute of Mineral Deposits, Chinese Academy of Geological Sciences, Beijing 100037, China*

BERND LEHMANN,\*

*Institute of Mineralogy and Mineral Resources, Technical University of Clausthal, 38678 Clausthal-Zellerfeld, Germany*

ANDAO DU,

*Institute of Rock and Mineral Analysis, Chinese Academy of Geological Sciences, Beijing 100037, China*

GUANGDI ZHANG,

*Institute of Mineral Deposits, Chinese Academy of Geological Sciences, Beijing 100037, China*

DONGSHENG MA,

*Department of Earth Sciences, Nanjing University, Nanjing 210008, China*

YITIAN WANG,

*Institute of Mineral Deposits, Chinese Academy of Geological Sciences, Beijing 100037, China*

MINGGUO ZENG,

*Institute of Geology, Guizhou Bureau of Geology, Mineral Resources, Exploration and Development, Guiyang 550002, China*

AND ROBERT KERRICH

*Department of Geological Sciences, University of Saskatchewan, Saskatoon, Canada S7N 5E2*

## Abstract

Black shales of the basal Lower Cambrian Niutitang Formation, southeast China, host a regionally distributed concordant, several centimeter-thick, sulfide layer which displays extreme metal enrichment, i.e., Mo-Ni-Se-Re-Os-As-Hg-Sb >1,000 times enriched and Ag-Au-Pt-Pd >100 times enriched over bulk continental crust. Mineable portions have about 5.5 wt percent Mo, 3.5 wt percent Ni, and 1 g/t PGE + Au. A six-point  $^{187}\text{Os}/^{188}\text{Os}$  versus  $^{187}\text{Re}/^{188}\text{Os}$  isochron on molybdenum-nickel ore samples defines an age of  $541 \pm 16$  Ma ( $2\sigma$ ) with an initial  $^{187}\text{Os}/^{188}\text{Os}$  ratio of  $0.78 \pm 0.19$ . This age is in agreement with the depositional age of the black shale host; the initial ratio is close to present-day seawater. The sulfide layer/average seawater metal ratio is on the order of  $10^6$  to  $10^8$ , about 10 to 100 times higher than that for the black shale host and for average metaliferous black shale. Syndimentary metal enrichment from seawater under anoxic (sulfate-reducing) conditions appears likely but requires an unusually low sedimentation rate and/or high replenishment rate of fresh seawater to the marine basin. The paleogeographic setting of the Lower Cambrian continental margin of the Yangtze craton indicates local basins controlled by syndimentary rifting. Stagnant water episodically replenished by upwelling oxidized seawater is thought to be responsible for the formation of the polymetallic sulfide layer and of phosphorite, barite, and sapropelic "stone coal" (combustible black shale) beds.

## Introduction

ORGANIC-RICH (black) shales from marine environments commonly contain higher amounts of molybdenum, nickel, vanadium, and a number of other metals than does any other sedimentary rock (Vine and Tourtelot, 1970). The enrichment factor of such elements in black shales compared to seawater is on the order of  $10^5$  to  $10^6$  and can be understood as a result of redox-controlled removal of trace metals from seawater in

anoxic bottom environments with a low sedimentation rate (Holland, 1979); however, certain stratigraphic subunits within black shale sequences display metal enrichment 10 to 100 times higher than that of average black shale, such as the classical 70-cm-thick Mecca Quarry Shale Member in the lower portion of the upper Carboniferous sequence of the midwestern United States (Coveney et al., 1987). The formation of such extremely metal-enriched portions of black shale sequences is commonly discussed in terms of diagenetic fluid flow (Coveney et al., 1987; Peacor et al., 2000) and/or hydrothermal metal input from submarine fluid venting during

\*Corresponding author: e-mail: lehmann@min.tu-clausthal.de

sedimentation (Loukola-Ruskeeniemi and Heino, 1996; Pasava et al., 1996).

The Lower Cambrian black shale sequence of the Niutitang Formation (and lateral equivalents) of southeastern China hosts a conformable polymetallic sulfide layer with an apparently unique and extreme case of metal enrichment (Fan Delian et al., 1973, 1984; Coveney and Chen, 1991; Coveney et al., 1992). The sulfide layer has about 10 wt percent organic matter and is extremely enriched in the element suite of Mo-Ni-Se-Re-Os-As-Hg-Sb (>1,000 times enriched over bulk continental crust) and Ag-Au-Pt-Pd (>100 times enriched over bulk crust) (Table 1). The thickness of the ore layer is commonly a few centimeters, with a continuous lateral extent of more than 1,000 m; occurrences of the sulfide layer at approximately the same stratigraphic level are known over a 1,600-km-long northeast trend which follows the paleocontinental margin of the Yangtze craton (Fig. 1a). The ore is locally mined and consists primarily of sulfides (mainly bravoite, vaesite, gersdorffite, and jordisite) and phosphates (francolite) that occur as nodular, polymictic, intraformational, flat pebblelike conglomerates and in laminated form. The same stratigraphic sequence also hosts huge barite deposits, as well as phosphorite and several meter-thick "stone

coal" beds of algal or planktonic origin (combustible black shale) which are mined (Coveney et al., 1994).

The extreme enrichment of the sulfide layer in nickel, molybdenum, and precious metals has been ascribed to a variety of processes, including hydrothermal input from fluids released into the basin during rifting (Coveney et al., 1992; Murowchick et al., 1994; Lott et al., 1999; Steiner et al., 2001), extraterrestrial impact origin (Fan Delian et al., 1984), and diagenetic fluid flow (Horan et al., 1994). A penecontemporaneous origin of sulfide mineralization and sedimentation has been suggested by earlier Re-Os isotope data which scatter around a reference isochron with an age of  $560 \pm 30$  Ma (Horan et al., 1994) and by a Pb-Pb age of  $551 \pm 52$  Ma (Murowchick et al., 1992).

The polymetallic sulfide layer is mined in the Huangjiawan mine, ca. 15 km west of Zunyi, Guizhou, where the thickness of the ore layer reaches up to 2 m (avg = 20 cm). The ore reserve at this locality is 240,000 t Mo + 150,000 t Ni and the grade is around 5.5 percent Mo, 3.5 percent Ni, and 1 g/t PGE + Au. In this study, seven samples were collected from the Huangjiawan mine for a geochemical reconnaissance study and for Re-Os isotope measurements in order to constrain the timing of this unusual black-shale hosted polymetallic mineralization better.

### Geologic Setting

The conformable polymetallic sulfide horizon occurs within the lowermost few meters of the up to >100-m-thick black shale sequence of the unmetamorphosed Niutitang Formation. The lower part of the Niutitang Formation hosts stratiform barite mineralization in the Gonxi district, Hunan (Wang and Li, 1991), massive phosphorite and manganese carbonate beds in the Tiantaishan district, Shaaxi (Hein et al., 1999), and up to a few tens of meters thick stone coal beds. The biostratigraphic age of the Niutitang Formation is constrained by a pretrilobitic (endemic) fauna consisting of bivalved arthropods (*Perspicaris*), sponges, and small shelly fossils which are considered to be of Tommotian age (about 530 Ma; Steiner et al., 2001).

The Niutitang Formation rests unconformably on a >100-m-thick carbonate sequence with karst features (Dengying Formation) which is attributed to the uppermost Sinian (terminal Neoproterozoic). The Dengying Formation is underlain, again following a stratigraphic hiatus, by the Doushantuo Formation, a mostly <100-m-thick black shale, chert, and dolomite sequence with V-Ag mineralization in some black shale units (Fan Delian et al., 1992). The Doushantuo Formation rests on tillites of the Nantuo Formation which is 590 to 575 Ma in age, when correlated with the global Marinoan-Varangerian glaciation (Brasier et al., 2000). The entire sedimentary sequence is thought to represent a sedimentary shelf environment characterized by repeated transgression-regression episodes on the Lower Proterozoic-Archean Yangtze craton (Qiu et al., 2000; Steiner, 2001; Steiner et al., 2001).

The Precambrian basement consists mainly of Proterozoic clastic metasedimentary rocks intercalated with mafic-ultramafic volcanic rocks; the upper section has been metamorphosed to the lower greenschist facies (Mao Jingwen, 1995). Mesozoic terrestrial cover rocks consist of red sandstone intercalated with Jurassic-Cretaceous andesites and rhyolites.

TABLE 1. Abundances of Selected Elements in Samples from the Huangjiawan Mine ( $n = 7$ ), in the Lower Cambrian Polymetallic Sulfide Layer of South China, in Upper Continental Crust, and in Average Seawater

Element	Huangjiawan mine (ppm)	Polymetallic sulfide layer (ppm)	Continental upper crust (ppm)	Seawater (ppt)
P	20,000	14,000	665	62,000
V	1,200	948	60	2,000
Cr	107	80	35	210
Mn	320	200	600	20
Fe	120,000	100,000	31,500	30
Co	185	50	10	1.2
Ni	36,000	26,000	20	480
Cu	2,600	650	25	150
Zn	2,950	1,600	71	350
As	17,000	10,000	1.5	1,200
Se	1,655	2,000	0.05	155
Mo	57,000	39,000	1.5	10,000
Ru	<0.010	0.023	0.0001	<0.005
Rh	0.020	0.025	0.00006	0.08
Pd	0.380	0.300	0.0005	0.06
Ag	75	50	0.005	2
Sb	550	360	0.2	200
Ba	800	1,900	550	15,000
W	n.a.	20	2	10
Re	11	6	0.0004	7.8
Os*	0.07	0.034	0.00005	0.002
Ir	0.003	0.0017	0.00002	0.00013
Pt	0.405	0.295	0.0015	0.05
Au	0.320	0.334	0.002	0.02
Hg	n.a.	25	0.012	0.14
Pb	504	100	20	2.7
U	140	200	2.8	3,200

Os\* is common Os (total Os minus radiogenic Os from  $^{187}\text{Re}$  decay)

Data sources: Fan Delian et al. (1984), Coveney et al. (1992), Horan et al. (1994), Steiner et al. (2001); average upper continental crust from GERM Reservoir Database (<http://www.earthref.org>), seawater from Nozaki (1997, [http://earth.agu.org/eos\\_elec/97025e.html](http://earth.agu.org/eos_elec/97025e.html)).

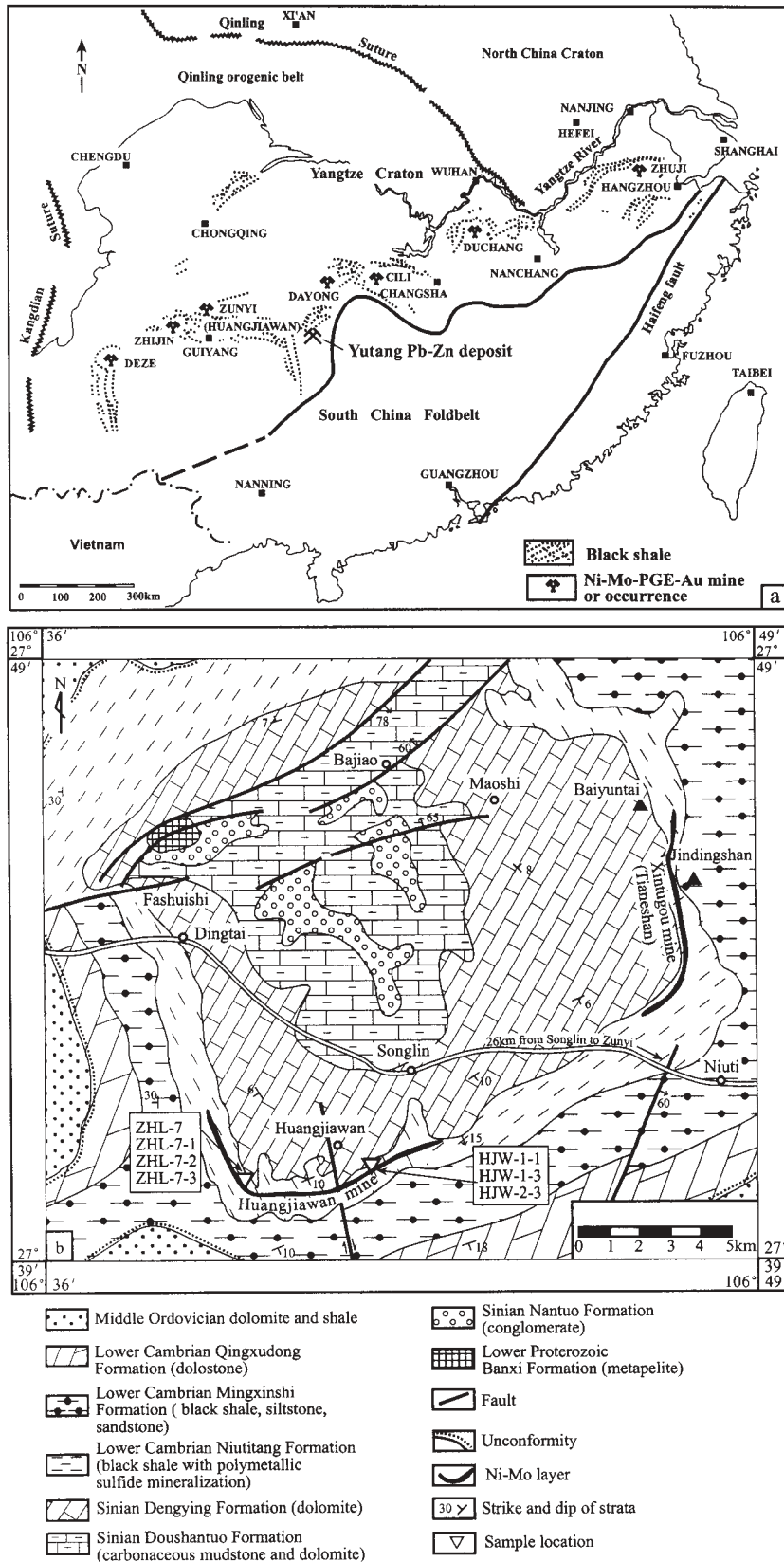


FIG. 1. a. Geotectonic setting and distribution of the Cambrian black shale in south China and related Ni-Mo-PGE-Au mines and occurrences. b. Geologic sketch map of the Songlin dome with location of the Huangjiawan mine and sampling sites (modified from Zeng Mingguo, 1998).

The Huangjiawan area has a gentle dome structure (Songlin dome) which exposes Neoproterozoic slate and metapelite in the center, surrounded by Sinian sediments (conglomerates of the Nantuo Formation, carbonaceous mudstone and dolomite of the Doushantuo Formation, and dolomite of the Dengying Formation), and the Early Paleozoic sediments of the Niutitang Formation (black shale), Mingxinshi Formation (carbonaceous mudstone), and Jindingshan Formation (siltstone) (Fig. 1b). The Lower Cambrian Qingxudong Formation (muddy dolomite) is overlain unconformably by Lower to Middle Ordovician clastic and carbonate rocks. There are no magmatic rocks exposed in the area. The larger east-northeast-, north-northeast-, and north-northwest-trending faults are of post-Early Paleozoic age; however, small-scale synsedimentary fractures (without hydrothermal infill) are abundant.

The Huangjiawan Ni-Mo-(PGE-Au) mineralization is confined to one single ore bed, as is also observed for all other known occurrences in the southeast China nickel-molybdenum belt. The ore deposit is located in the southern portion of the Songlin dome and has a lateral equivalent in the abandoned Xintugou (Tianeshan) mine area to the east (Fig. 1b). The ore-bearing Niutitang Formation can be divided into six lithological units from the bottom upward, as follows (Zeng Mingguo, 1998):

1. An iron-manganese oxide-rich weathering crust which occurs in discontinuous lenses on the undulating paleosurface of the Sinian Doushantuo dolomite (0–0.3 m in thickness).

2. A brownish to black uranium-rich phosphorite material intercalated with lenses of dolomite (about 0.5 m in thickness). The stratigraphic equivalent of this unit is mined for phosphate in certain localities and there can reach several meters in thickness.

3. An organic carbon-rich hydromica claystone-shale intercalated with lenses of phosphorite or phosphatic nodules. Collophane contains 200 to 300 ppm U, and the concentration of Mo, Ni, V, Y, and light REE in the claystone locally reaches economic grade. This layer is about 0.5 to 2.5 m thick.

4. An Ni-Mo-PGE-Au-bearing sulfide ore bed, locally disrupted sulfide microlenses, and flat pebblelike conglomerates. Contacts with overlying and underlying units are sharp. The ore bed is continuous over a several-kilometer strike length with a thickness of 5 to 30 cm on average in the eastern part, and 20 to 50 cm in the western part. The maximum thickness is 2 m. The Ni-Mo sulfides occur laminated (Fig. 2a), in pods, and with nodular textures (Fig. 2b-f) within carbon-rich hydromica claystone-shale.

5. Organic carbon-rich hydromica claystone-shale, known as the Mo-V-bearing stone coal layer. This layer has up to 35 wt percent  $C_{\text{organic}}$  and contains 0.1 to 0.3 wt percent Mo, 0.05 to 0.2 wt percent Ni, and 0.05 to 0.9 wt percent V.

6. Carbonaceous hydromica claystone-shale (>100 m in thickness).

Detailed stratigraphic information and measured sections of the terminal Neoproterozoic to Cambrian boundary in south China can be found in Steiner (2001), Steiner and Erdtmann (2001) and Steiner et al. (2001).

The ore consists of laminated metal-rich material and polymictic intraformational nodules. The nodules are <1 to 3

mm long and occur as a mixture of heterogeneous microcrystalline assemblages of Fe, Mo, and Ni sulfides and a colloid-like Mo-S-C phase (Fig. 2), together with organic debris, quartz, carbonates, clay minerals, and apatite. The main host for molybdenum is an amorphous to weakly crystalline Mo-S-C mixed layer phase which recently was identified with the approximate formula  $(\text{Mo,Fe,Ni})_3(\text{S,As})_6\text{C}_{10}$  (Kao et al., 2001). The Ni-Mo-rich colloidal aggregates (or nodules) are ellipsoidal or spherical in shape and show recrystallization to very fine grained mineral assemblages around nodule margins or along fractures (Fig. 2). Nickel occurs mainly in vaesite and bravoite dispersed through the colloidal Mo-S-C nodules. Ni-bearing pyrite is the most abundant sulfide mineral; minor ore minerals are millerite, gersdorffite, chalcopyrite, sphalerite, tennantite, and covellite. The proportion of sulfide minerals to the Ni-Mo-rich colloidal nodules is about 1 to 4–5, with the sulfide mineral proportion increasing from the bottom upward in the ore bed.

There are also sulfide microveinlets occurring among or cutting through the colloidal nodules. All ore minerals are anhydrous. Gangue minerals in the ore bed are hydromica, illite, sericite, quartz, calcite, barite, apatite, and collophane. Pyrobitumen is abundant and occurs in wavy laminations and knots ( $C_{\text{organic}}$  up to 11 wt %). The ore contains abundant microfossils (cyanobacteria, acritarchs, algae, sponges; Murowchick et al., 1994; Lott et al., 1999; Steiner et al., 2001).

The organic-rich, claystone-shale footwall of the ore layer has locally abundant barite and gypsum (Coveney et al., 1993), as well as phosphorite concretions. The abundance of V and Cr is about 10 times higher than that of the polymetallic sulfide layer, whereas Ni and Mo are about 10 times less abundant than that of the sulfide layer. Microfossil material is abundant and sulfide replacement of microbial mats within the sulfide layer is common. Highly variable  $^{34}\text{S}$  values and fine-scale cyclic variations (SHRIMP  $\delta^{34}\text{S}$  data of  $-26$  to  $+22\text{‰}$  over a 0.2-mm distance in a pyrite nodule) point to bacterial sulfate reduction under conditions of sulfur limitation (Murowchick et al., 1994).

### Re-Os Isotope Analysis

Seven 1- to 5-kg bulk ore samples from the Huangjiawan mine were analyzed (Tables 2 and 3). The samples are from fresh open-pit mining faces and were crushed, split, and ground to <100- $\mu\text{m}$  grain size. The isotope analyses were done in the Re-Os laboratory of the National Research Center of Geoanalysis, Chinese Academy of Geological Sciences, Beijing. Enriched  $^{190}\text{Os}$  and enriched  $^{185}\text{Re}$  were obtained from the Oak Ridge National Laboratory. The standard reagents  $(\text{NH}_4)_2\text{OsCl}_6$  and  $\text{NH}_4\text{ReO}_4$  for calibration of spikes were spectroscopically pure products of the Johnson Matthey Company of Great Britain. These were dissolved in HCl to produce standard solutions (Du Andao et al., 1995).

A Carius tube digestion was used (Shirey and Walker, 1995) whereby a ~0.1-g sample is loaded in a thick-walled borosilicate glass ampoule together with  $^{190}\text{Os}$  and  $^{185}\text{Re}$  spike solutions and 6 ml of 15 M  $\text{HNO}_3$  and 2 ml of 12 M HCl. While the bottom part of the tube is frozen, the top is sealed using an oxygen-propane torch. The tube is then placed in a stainless steel jacket and heated for 12 h at 230°C. Upon cooling, the tube is immersed in an ethanol-dry ice slush, the neck of

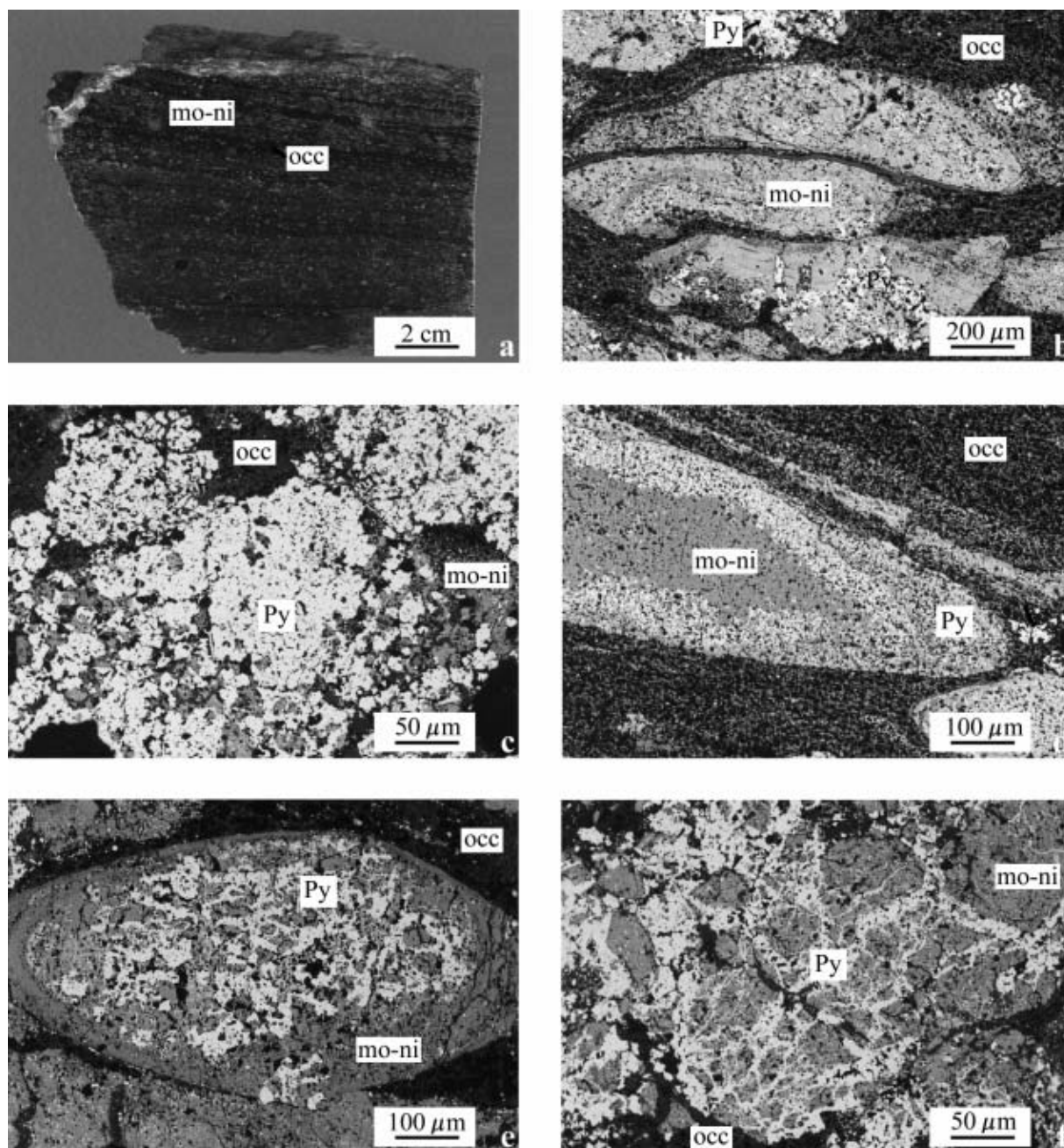


FIG. 2. Photographs of polished Ni-Mo ore samples (plane light) from the Huangjiawan mine. Abbreviations: mo-ni = colloidal molybdenum- and nickel-rich sulfide nodules; occ = organic carbonaceous material; Py = pyrite. a. Laminated fabric of Ni-Mo-rich sulfide nodules (gray) intercalated with carbon-rich hydromica claystone (dark). b. Colloidal Ni-Mo-rich sulfide nodules (light) and pyrite in carbon-rich hydromica shale and clastic debris (dark). c. Recrystallized pyrite and Ni-bearing pyrite in colloidal Ni-Mo-S nodules. d. Recrystallized fine-grained pyrite in rim zones of colloidal Ni-Mo-S nodules. e. Fine-grained pyrite intergrown with colloidal Ni-Mo-S phase. f. Pyrite microveinlets in Ni-Mo-S nodules.

the tube is broken, and the contents of the tube are poured into a distillation flask and the residue washed out with 40 ml of deionized (18 M $\Omega$ ) water.

The Os is separated by distillation as OsO<sub>4</sub> three times. In the first distillation step, OsO<sub>4</sub> is trapped in 10 ml of water. The residual Re-bearing solution is saved for Re separation. The water trap solution plus 40 ml of water is distilled a second time. The OsO<sub>4</sub> is trapped in 5 ml of 8 M ultrapure HBr,

and the Os-bearing HBr solution is kept for 4 h at 80°C. The trap solution is transferred to a Teflon vial for microdistillation (Birck et al., 1997). The last trap solution of 10  $\mu$ l of HBr is used for negative thermal ion mass spectrometry (NTIMS) by a Finnigan Mat-262 instrument.

The Re-bearing solution is evaporated to dryness, 1 ml of water added, and then heated to near-dryness twice. Ten milliliters of 20 percent NaOH are added to the residue solution,

TABLE 2. Chemical Data for Black-Shale Sample Set (Bulk Rock) Analyzed for Re-Os Isotopes

Sample no.	C <sub>organic</sub> (wt %)	Fe (wt %)	Ni (wt %)	Mo (wt %)	Mn (ppm)	Cu (ppm)	V (ppm)	U (ppm)	Pt (ppb)	Pd (ppb)
HJW-1-1	11.4	13.15	3.35	3.71	360	2,240	921	287	406	347
HJW-1-3	10.2	10.62	2.33	4.06	336	2,260	1,020	105	337	291
HJW-2-3	10.3	13.40	4.05	4.24	322	3,770	992	120	477	451
ZHL-7	11.1	12.71	3.39	3.98	292	2,690	852	168	460	446
ZHL-7-1	13.4	11.68	3.90	9.29	331	2,690	1,940	52	360	338
ZHL-7-2	12.1	10.97	4.78	7.68	193	2,290	1,390	93	386	403
ZHL-7-3	12.0	12.48	3.67	7.06	385	2,280	1,310	158	408	408

Pt and Pd data from Ni sulfide fire assay with ICP-MS finish (error is estimated at <10%), C<sub>organic</sub> by Leco carbon analyzer, other elements by ICP-AES after acid digestion (HCl-HNO<sub>3</sub>-HF-HClO<sub>4</sub>); all analyses at the National Research Center of Geoanalysis, Beijing

TABLE 3. Re and Os Abundances, Isotope Ratios, and Model Ages for Ore Samples from the Huangjiawan Mine, Guizhou

Sample no.	Weight (g)	Re ( $\mu\text{g/g}$ )	Total Os (ng/g)	<sup>187</sup> Re/ <sup>188</sup> Os	<sup>187</sup> Os/ <sup>188</sup> Os	Model age (Ma)
HJW-1-1	0.10103	10.438(42)	133.92(54)	731.2(4.2)	7.397(14)	541 (15)
HJW-1-3	0.10079	10.268(41)	124.35(50)	813.3(4.6)	8.141(15)	541 (14)
HJW-2-3	0.10060	12.682(51)	162.14(65)	736.5(4.2)	7.451(14)	541 (15)
ZHL-7	0.10343	10.901(44)	142.30(57)	700.9(4.0)	7.027(13)	534 (16)
ZHL-7-1	0.10055	12.193(49)	156.76(63)	726.3(4.1)	7.326(14)	539 (15)
ZHL-7-2	0.10156	11.358(45)	152.76(61)	673.2(3.8)	6.876(13)	541 (17)
ZHL-7-3	0.10021	10.856(43)	142.05(57)	705.9(4.0)	7.165(13)	541 (16)

Absolute uncertainties ( $2\sigma$ ) are shown in the last digits in parentheses; uncertainty includes errors in (1) <sup>185</sup>Re and <sup>190</sup>Os spike calibrations, 0.1% ( $2\sigma$ ), (2) magnification with spiking, (3) mass spectrometric measurement of isotopic ratios; model age is calculated with an initial <sup>187</sup>Os/<sup>188</sup>Os of 0.78 and an <sup>187</sup>Re decay constant of  $1.666 \times 10^{-11} \text{ yr}^{-1}$  (Smoliar et al., 1996)

followed by Re extraction with 10 ml of acetone. Two milliliters of water is added to the Re-bearing acetone solution that is evaporated to dryness and picked up in 5 ml of 0.8 M HNO<sub>3</sub>. Small anion exchange columns are prepared according to Markey et al. (1998). About 2 ml of this solution is loaded on a 0.2-ml anion exchange column (AG-1  $\times$  8, 200–400 mesh resin) followed by a mix of 3 ml of 0.8 M HNO<sub>3</sub>, 3 ml of 1 M HCl, and 1 ml of water to wash impurity elements. Three milliliters of 4 M HNO<sub>3</sub> is used to elute Re that is dried-down to one drop for mass spectrometer determination (Markey et al., 1998). Single Pt filaments (EHPI or CROSS) were used. Filament loads are ~30 ng Re and ~10 ng Os, applied with 10  $\mu\text{g}$  Ba (as barium nitrate) and 2  $\mu\text{g}$  Na (as sodium hydroxide). For both Re and Os, at least five blocks of analyses comprising 10 scans each are cumulated.

Average blanks for the total Carius tube procedure as described above are ca. 20 pg Re and ca. 7 pg Os with <sup>187</sup>Os/<sup>188</sup>Os of 0.81 to 1.4. The analytical reliability was tested by repeat analyses of molybdenite standard HLP-5 from a carbonatite vein-type molybdenum-uranium deposit in the Jinduicheng-Huanglongpu area of Shaanxi Province, China. Seventeen samples were analyzed over a period of six months. The uncertainty in each individual age determination is about 0.7 percent including the uncertainty of the decay constant of <sup>187</sup>Re, uncertainty in isotope ratio measurement, spike calibrations, and spike weighing errors. The average Re-Os age on HLP-5 was  $221.3 \pm 0.3 \text{ Ma}$  (95% confidence limit). Median age and mean absolute deviation were  $221.34 \pm 0.12 \text{ Ma}$  (Du Andao et al., 2001). The same reference material is also used by the AIRIE Group, Fort Collins, Colorado (Stein et al., 1997). They produced a median age of  $221.30 \pm 0.24 \text{ Ma}$

on 19 analyses run over a period of 18 months (Markey et al., 1997).

The decay constant used for <sup>187</sup>Re of  $1.666 \times 10^{-11} \text{ yr}^{-1}$  has an absolute uncertainty of about  $\pm 1$  percent (Smoliar et al., 1996); however, this error is probably smaller, given the results by Shen et al. (1996) and Birck and Allègre (1998) which agree within  $\pm 0.4$  percent of the value reported by Smoliar et al. (1996).

## Results and Discussion

Seven bulk ore sample powders were analyzed for Re and Os isotopes (Table 3) and a number of major and trace elements (Tables 1 and 2). Six of the seven samples define an isochron age of  $541 \pm 16$  ( $2\sigma$  Ma with an initial <sup>187</sup>Os/<sup>188</sup>Os ratio of  $0.78 \pm 0.19$ ; MSWD = 0.46; Fig. 3). The model ages for the ore samples are mostly within the range of 541 to 539 Ma, with one sample (ZHL-7) at 534 Ma, which was not included in the isochron calculation. The low MSWD implies little scatter, much different from the earlier study of Horan et al. (1994). Note, however, that our sample suite is from only two locations about 5 km apart, with samples taken over an outcrop length of about 20 m in each locality.

The initial <sup>187</sup>Os/<sup>188</sup>Os ratio of  $0.78 \pm 0.19$  is similar to that of other black shales and pelagic clay (Ravizza and Turekian, 1989), but the sample powders are less radiogenic than present-day upper continental crust samples from loess and deltaic sediments (<sup>187</sup>Os/<sup>188</sup>Os = 1.8–2.4; Esser and Turekian, 1993). Their ratio is also slightly different from the initial <sup>187</sup>Os/<sup>188</sup>Os ratio of  $1.18 \pm 0.02$  recently obtained on Lower Cambrian black shale samples in the Lesser Himalaya, India (Singh et al., 1999).

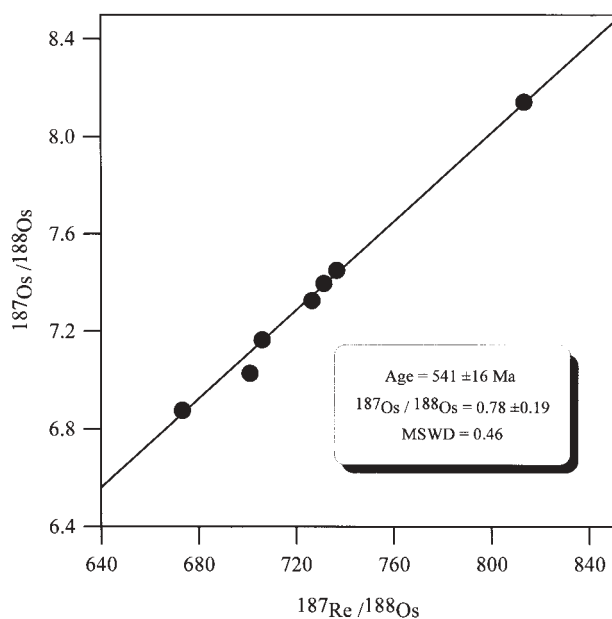


FIG. 3. Re-Os isochron plot of Ni-Mo-(PGE-Au) ore samples from the Huangjiawan mine. ISOPLOT software (model 1) was used to calculate the isochron age. The regression is based on six points (solid dots), excluding sample ZHL-7 (shaded circle). Error bars are smaller than the symbols.

The new Re-Os isochron age refines the earlier estimate of Horan et al. (1994) who found a scatter distribution along a reference line of 560 Ma, assuming a minimum initial  $^{187}\text{Os}/^{188}\text{Os}$  of 0.12, similar to that of carbonaceous chondrites and mantle at that time. Our new isochron age of  $541 \pm 16$  Ma suggests that molybdenum ore formation was synchronous with the black shale sedimentation. The initial  $^{187}\text{Os}/^{188}\text{Os}$  ratio of  $0.78 \pm 0.19$  is similar to that of present-day metalliferous pelagic sediments but slightly lower than that of present-day average seawater which has  $^{187}\text{Os}/^{188}\text{Os} = 1.04 \pm 0.04$  (Sharma et al., 1997). The Os isotope composition of seawater is controlled by continental runoff ( $^{187}\text{Os}/^{188}\text{Os} > 1.2$ ), hydrothermal input from seawater circulating through the oceanic crust ( $^{187}\text{Os}/^{188}\text{Os} = 0.1$ ), and contributions from cosmic dust ( $^{187}\text{Os}/^{188}\text{Os} = 0.1$ ; Sharma et al., 1997). Pelagic clays from the North Pacific have been interpreted to indicate a  $^{187}\text{Os}/^{188}\text{Os}$  variation in seawater of 1.0 to 0.3 for the last 58 m.y. (Pegram et al., 1992). It appears that the continental osmium component was less important in the polymetallic sulfide layer than in the present-day oceans, but it is still within the variation range of seawater with geologic time.

One data point (ZHL-7) from the seven sample set falls to the right of the isochron, indicating that Re and/or Os in this sample was mobile at some time after deposition. Remobilization of Re and Os on a small scale could be the result of variable interaction with ground water over an extended diagenetic history or of weathering (Hannah et al., 2001); however, we could not detect any textural or mineralogical differences between sample ZHL-7 and the remaining sample set. The much larger data scatter in the earlier study by Horan et al. (1994) may be due to analytical problems in the early stage of Re-Os geochronology, i.e., incomplete equilibration of spike and sample or too small a sample size. Also, the samples

from the study by Horan et al. (1994) were from different localities several hundred kilometers apart. Given that deposition was occurring on a continental margin with highly restricted basins, a slight spatial variation in the initial  $^{187}\text{Os}/^{188}\text{Os}$  along the shelf might be anticipated.

The age of  $541 \pm 16$  Ma for the sulfide layer is very close to the currently accepted Precambrian-Cambrian boundary of ca. 544 Ma (Bowring et al., 1993; Landing et al., 1998), which suggests a Manykaian age for the polymetallic mineralization; however, the error range also includes the Tommotian stage (around 530 Ma) which was proposed as depositional age of the Niutitang Formation based on biostratigraphic evidence (Steiner et al., 2001).

The Re-Os age and the initial  $^{187}\text{Os}/^{188}\text{Os}$  ratio close to present-day seawater suggest a synsedimentary ore formation and a dominantly seawater source for the Re and Os. Rhenium and Os can be scavenged efficiently by anoxic bottom sediments (Ravizza et al., 1991) and are typically enriched in black shales; however, most of the researchers who have worked on the south China Lower Cambrian sulfide layers attribute the extreme metal enrichment to hydrothermal vents or seepages, with leaching of metals from deeper sources (Coveney et al., 1992; Murowchick et al., 1994; Lott et al., 1999; Steiner et al., 2001). Sedimentary-exhalative deposits, however, commonly have a Cu-Pb-Zn sulfide assemblage, not the more unusual enrichment of Ni, Mo, Re, and PGE seen in the polymetallic sulfide layer. The wide lateral extent of the thin sulfide layer over hundreds of kilometers in southern China contrasts with the lenticular shape of exhalative deposits, which are usually located near hydrothermal vents and are continuous over only a few kilometers, at most (Large, 1976).

Hydrothermal vent deposits have not been found in the Lower Cambrian of southern China. Lott et al. (1999) report fluid inclusion data from quartz-carbonate-fluorite-barite veinlets ( $\pm$  base metal sulfides) from the underlying Proterozoic dolostone sequence. The fluid inclusions consist of basinal brines (up to 22 wt % NaCl equiv) with homogenization temperatures in the  $60^\circ$  to  $190^\circ\text{C}$  range and were interpreted by Lott et al. (1999) as representative of the fluid system which possibly vented at the sea bottom farther up in the stratigraphic sequence and produced the polymetallic sulfide layer. Such fluid systems with basinal brine characteristics, however, are known from all sedimentary basins, including those in southern China (Liu et al., 1997). Large-scale basinal brine circulation in the study area is indicated by widespread collapse breccia in Proterozoic and Cambrian limestone-dolostone units with traces of galena-sphalerite-fluorite-barite mineralization (our own field observations), and by the Mississippi Valley-type strata-bound Pb-Zn ore deposits (Yutang mine) of the Huayuan district in Hunan, found in Lower Cambrian limestone about 80 km south of Dayong (Zhou et al., 1983; Peng, 1986; Liu et al., 1997; Boni et al., 2001). Fluid inclusions from the Huayuan district have homogenization temperatures in the range of  $100^\circ$  to  $180^\circ\text{C}$  and typical basinal brine salinities up to 34 equiv wt percent NaCl (Liu et al., 1997). Lott et al. (1999) did their fluid inclusion study on quartz-fluorite veinlets in the same general geographic and stratigraphic setting as that of Huangjiawan, but we do not think that their study relates to the fluid system responsible

for the formation of the polymetallic sulfide layer. We therefore would not agree with the conclusions of Lott et al. (1999) who propose an exhalative-hydrothermal model for the formation of the polymetallic sulfide layer, and we favor a dominantly marine origin for this unusual metal enrichment.

Figure 4 compares element distribution patterns for upper continental crust, seawater, and the Lower Cambrian sulfide layer in south China. The primitive mantle-normalized PGE patterns of the sulfide ore show a terrestrial fractionation pattern not compatible with significant mixing of a chondrite component. Further evidence against an extraterrestrial chemical input are the high U, Sb, As, Mo, Se, and Re abundances.

The ore layer displays a relatively constant enrichment factor compared to that of seawater on the order of  $10^6$  to  $10^8$  for PGEs, Au, Ag, Re, Se, V, As, Sb, Co, Pb, Hg, Re, W, Sb, Zn, Ni, and Mo (Fig. 5, Table 1). The ore layer is about an order of magnitude less enriched in the element group Cr-V-U-Ba-P. The enrichment of the black shale host sequence is similar to that of the average metalliferous black shale, with an enrichment factor of  $10^5$  to  $10^6$  for these elements (not shown; compare Holland, 1979). Holland (1979) demonstrated that, in a stagnant basin, the enrichment factor R (concentration of element i in rock sample/concentration of element i in seawater) is related to height of water column (h), water density ( $\rho$ ), sediment accumulation rate ( $\omega$ ), and the rate of replenishment by fresh sea water (every  $\tau$  years):

$$R = (h \cdot \omega) / \rho \cdot \tau.$$

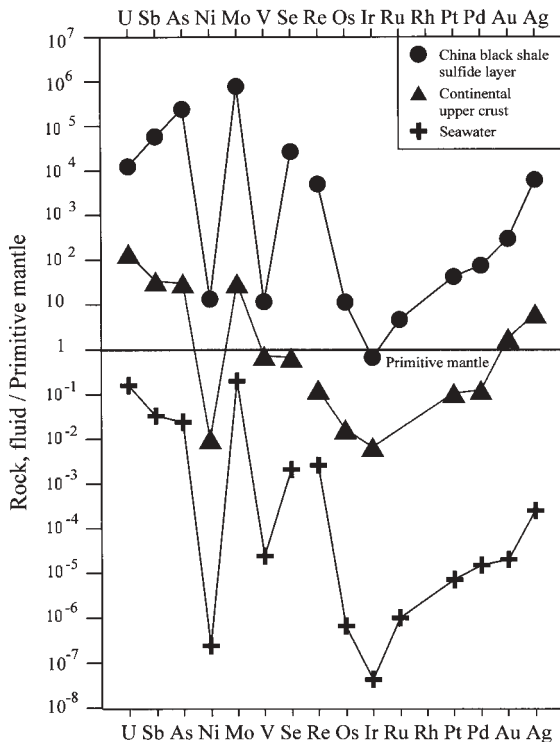


FIG. 4. Multi-element plot, normalized to primitive mantle, for average composition of south China sulfide layer compared to seawater and upper continental crust. Data sources for sulfide layer: Fan Delian et al. (1984), Coveney et al. (1992), Horan et al. (1994), and Steimer et al. (2001). Seawater data from Nozaki (1997, [http://earth.agu.org/eos\\_97025e.html](http://earth.agu.org/eos_97025e.html)), primitive mantle and upper continental crust from GERM Reservoir Database (<http://www.earthref.org>).

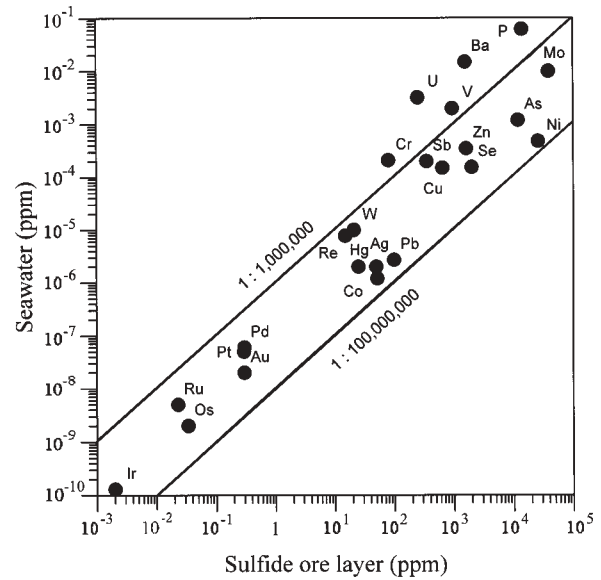


FIG. 5. Element abundances in the polymetallic sulfide layer versus average seawater (data sources as for Fig. 4).

Holland (1979) demonstrated that metalliferous black shales can reach the observed enrichment factor of  $5 \times 10^5$  for a model of a 1,000-m deep anoxic basin with a replenishment rate once every 1,000 years, and if sediment is deposited within the basin at a rate of  $0.2 \text{ mg cm}^{-2} \text{ yr}^{-1}$ . A 10 to 100 times higher enrichment factor in the ore layer could be understood as a consequence of a particularly low sedimentation rate, a particularly short replenishment period, and/or metal-enriched seawater.

The study by Jacobs et al. (1987) on molybdenum in the Cariaco trench (off Venezuela) can be used as an example for present-day metal enrichment in anoxic basins. The Cariaco trench has an anoxic (sulfate-reducing) water column of 1,000 m with a bottom-water residence time of 100 to 200 years. The amount of molybdenum in the seawater is 10 ppb (Collier, 1985) which gives a flux of seawater Mo into the basin of 5 to  $10 \mu\text{g cm}^{-2} \text{ yr}^{-1}$ . The proximity of the Cariaco trench to major rivers of northern South America causes a high bulk sedimentation rate of around  $100 \text{ mg cm}^{-2} \text{ yr}^{-1}$ . As a result of the high influx of terrigenous material, the absolute molybdenum concentration in the Cariaco trench sediments is only 50 to 100 ppm Mo (Jacobs et al., 1987); however, for a low sedimentation rate on the order of a few tenths of  $\text{mg cm}^{-2} \text{ yr}^{-1}$ , molybdenum would be much less diluted and would reach the percent level.

Metal fixation by living organisms is unlikely to have contributed significantly to the metal enrichment because interelement relations in marine plankton (Brumsack, 1986; Piper, 1994) show ratios very much different from the metal ratios in the sulfide layer, and such material also would have much more phosphorus than heavy metals. The strong discrepancy between Cu/Zn/Se/Ni/Mo ratios of 6:55:2:4:1 in plankton (Piper, 1994) compared to approximately 1:3:3:40:60 in the sulfide layer (Table 1) makes it unlikely that a significant fraction of the heavy metals might have accumulated as biogenic debris (Piper, 1994).

On the other hand, the high amount of organic carbon in the sulfide layer indicates high biogenic accumulation, and the redox reactions driven by this organic background could directly precipitate redox-sensitive metals from  $O_2$ -depleted bottom water (Holland, 1979; Piper, 1994). The comparison of the element distribution patterns of seawater and the sulfide layer (Fig. 5), and the interelement ratios with Cu/Zn/Se/Ni/Mo proportions of 1:2:1:3:65 in seawater compared to 1:3:3:40:60 in the sulfide layer support this suggestion, although the Ni concentrations indicate an additional fractionation mechanism, most likely changing redox conditions. The chemical properties of bottom water change in response to seawater advection, and sampling inevitably averages ocean conditions over thousands of years of deposition. Given a modest sedimentation rate of  $0.2 \text{ mg cm}^{-2} \text{ yr}^{-1}$ , a shale sample 1 cm thick will represent more than 10,000 years of deposition. Thus, a single sample may record highly variable bottom-water redox conditions.

The redox state of deep seawater is determined by bacterial oxidation of organic matter and proceeds in a sequence of oxidation from oxygen respiration to denitrification and on to sulfate reduction during which, first,  $O_2$  is consumed, then nitrate, and, eventually, sulfate (Froelich et al., 1979). As  $O_2$  is renewed in bottom water by advection, the type of respiration which occurs within the bottom water of a basin represents a balance between the rate at which organic matter settles out of the photic zone and bottom-water residence time. The behavior of redox-sensitive metals will be controlled by these changing conditions of bacterial respiration. For example, vanadium under oxic conditions is in the  $H_2VO_4^-$  state and is reduced to a less soluble valence state at the low Eh boundary of denitrification, whereas the reduction of  $CrO_4^{2-}$  occurs at the upper Eh boundary of denitrification (Piper, 1994). A series of studies of elemental distributions in marine basins in which present-day sulfate reduction occurs in bottom waters (such as the Cariaco trench or the Black Sea) have shown that the associated sediments are a major sink for elements such as Mo, Ni, Se, and U (see compilation in Piper, 1994). Since the concentration of Mo in seawater is much higher than that of any other heavy metal (Collier, 1985), molybdenum enrichment in marine sediments is a diagnostic feature of sulfate-reducing conditions in the bottom water at the time of deposition (Jacobs et al., 1987).

In the Cariaco trench and the Black Sea, the entire sulfate-reducing portion of the seawater column contributes to the accumulation of the hydrogenous fraction of molybdenum in the sediments (Jacobs et al., 1987; Piper, 1994). This finding suggests that precipitation and/or adsorption onto settling particulate matter, rather than diffusion across the benthic boundary, is the dominant mechanism of metal fixation, also corroborated by the lack of a concentration gradient in the sediment interface below anoxic water columns (Piper, 1994).

The black shale sequence at the Huangjiawan mine displays elevated U, V, Cr, Ba, and P abundances in the footwall, which are up to one order of magnitude higher than in the sulfide layer. This difference in trace element abundance can be understood as a result of redox conditions which, in the footwall zone, appear to correspond to denitrifying conditions (i.e., fixation of V and Cr), whereas the high Mo-Ni signature in the sulfide horizon reflects anoxic sulfate-reducing conditions.

Downward remobilization of many elements, including Re, U, Se, Hg, and Mo, is often observed in recent suboxic environments, where these elements are dissolved in the uppermost oxidized sediments and then concentrated at or below the oxidation front (Thomson et al., 1993; Mercone et al., 1999; Crusius and Thomson, 2000). This oxidative mobilization and reconcentration in deeper sediments, spanning meters of depth, could be an important enrichment process when a reducing sediment lies exposed to bottom water  $O_2$  at a low sediment accumulation rate. This process also could provide locally metal-enriched seawater, particularly in a restricted near-shore environment. We do not have the data necessary from geochemical profiles to discuss such a process; however, an oxic-suboxic boundary which should be expressed in a color change, is not observed and data on overlying and underlying black shale units indicate consistently high metal contents (ca. 50–100 ppm Mo; Steiner et al., 2001).

We therefore favor a model of water-column scavenging similar to that of present-day sulfate-reducing environments such as the Black Sea and the Cariaco trench, where Mo-enriched sediments underlie Mo-depleted water columns (Jacobs et al., 1987; Emerson and Husted, 1991; Helz et al., 1996). Sulfate reduction produces hydrogen sulfide which probably plays a key role in the change of the marine behavior of molybdenum from a conservative element to that of a particle-reactive element (Helz et al., 1996). At seawater pH, the concentrations of  $[MoO_4]^{2-}$  and  $[MoS_4]^{2-}$  are equal at  $\alpha_{HS^-} = 10^{-3.6}$  (pH 8.3) or  $10^{-4.3}$  (pH 7.5), and the sharpness of the transition from molybdate to tetrathiomolybdate species indicates that  $HS^-$  acts as a geochemical switch (Helz et al., 1996). Since  $HS^-$  concentrations in natural anaerobic waters range to values above  $10^{-3} \text{ M}$ , the  $\alpha_{HS^-}$  switch will be activated in many such environments. The sulfidation of hard-ligand  $[MoO_4]^{2-}$  dramatically alters the geochemical behavior of molybdenum because thiomolybdates and intermediate oxythiomolybdates are soft ligands that are reactive with many transition metals and organic matter. Both iron compounds and organic debris are known to be extremely efficient scavenging agents in sulfidic water columns (Helz et al., 1996), and X-ray amorphous Fe-Mo-S and Mo-S-C cluster compounds have been identified in the southeast China sulfide layer. The presence of these compounds attests to their stability over long geologic time periods (Helz et al., 1996; Kao et al., 2001).

## Conclusions

Geologic setting and ore textures suggest a syngenetic marine origin of the polymetallic sulfide layer in the Lower Cambrian black shale sequence of south China. The new Re-Os isochron age of  $541 \pm 16 \text{ Ma}$  supports the field and petrographic observations, i.e., congruency of bedding and mineralization at the kilometer to millimeter scale. The interelement pattern of the polymetallic sulfide layer is basically similar to that of average seawater and displays an enrichment factor of  $10^6$  to  $10^8$  for a broad redox-sensitive element spectrum. Although this enrichment factor is high, strong metal enrichment by precipitation-scavenging from average seawater is possible. Such a process requires a very low sedimentation rate and replenishment of a stagnant basin by fresh seawater on a time scale of hundreds of years.

Synsedimentary block tectonics, sulfide clast pebble horizons, second-order stone coal (sapropelic alginite) basins, synsedimentary barite and phosphorite deposits, and the general position of the polymetallic sulfide layer along the passive continental margin of the Yangtze craton, point to paleogeographic conditions of stagnant water basins which were episodically replenished by upwelling oxidized seawater.

### Acknowledgments

We thank Liu Xuanfeng and Feng Xueshi for their kind help during our field investigation. We are grateful to Wang Shuxian, Sun Dezhong, and Zhang Zuoheng for assistance during laboratory work. This study was granted by the Major State Basic Research Program of the People's Republic of China (G1999043211) and is also a first contribution to the new Sino-German Cooperative Program on "From Snowball Earth to the Cambrian Bioradiation: A Multidisciplinary Analysis of the Yangtze Platform, China," funded by the Natural Science Foundation of China and Deutsche Forschungsgemeinschaft. The authors are indebted to the three journal reviewers, Robert Creaser, Judith Hannah, and Edward Ripley, as well as to the two editors, Marco Einaudi and Mark Hannington, whose critiques helped improve this paper.

March 7, 2001; February 18, 2002

### REFERENCES

- Birck, J.L., and Allègre, C.J., 1998, Rhenium-187-osmium-187 in iron meteorites and the strange origin of the Kodaikanal meteorite: *Meteoritics and Planetary Science*, v. 33, p. 647-653.
- Birck, J.L., Roy Barman, M., and Capmas, F., 1997, Re-Os isotope measurements at the femtomole level in natural samples: *Geostandards Newsletter*, v. 20, p. 19-27.
- Boni, M., Lapponi, F., Schneider, J., Bechstdt, T., Liu, W., and Zheng, R., 2001, A preliminary Pb-Pb and U-Pb study on the MVT ore deposits in the Cambrian of Hunan (south China): SGA-SEG Joint Biennial Meeting, Krakow, Poland, August 26-29, 2001, Proceedings, p. 117-120.
- Bowring, S.A., Grotzinger, J.P., Isachsen, C.E., Knoll, A.H., Pelechaty, S.M., and Kolosov, P., 1993, Calibrating rates of Early Cambrian evolution: *Science*, v. 262, p. 1293-1298.
- Brasier, M., McCarron, G., Tucker, R., Leather, J., Allen, P., and Shields, G., 2000, New U-Pb zircon dates for the Neoproterozoic Ghubrah glaciation and for the top of the Huqf Supergroup, Oman: *Geology*, v. 28, p. 175-178.
- Brumsack, H.J., 1986, The inorganic geochemistry of Cretaceous black shales (DSDP Leg 41) in comparison to modern upwelling sediments from the Gulf of California, in Summerhayes, C.P., and Shackleton, N.J., eds., *Facets of modern biogeochemistry*. Festschrift für E.T. Degens: Berlin, Springer, p. 326-352.
- Collier, R.W., 1985, Molybdenum in the northeast Pacific Ocean: *Limnology and Oceanography*, v. 30, p. 1351-1354.
- Coveney, R.M., Jr., and Chen, N.S., 1991, Ni-Mo-PGE-Au-rich ores in Chinese black shales and speculations on possible analogues in the United States: *Mineralium Deposita*, v. 26, p. 83-88.
- Coveney, R.M., Jr., Leventhal, J.S., Glascock, M.D., and Hatch, J.R., 1987, Origins of metals and organic matter in the Mecca Quarry Shale Member and stratigraphically equivalent beds across the Midwest: *ECONOMIC GEOLOGY*, v. 82, p. 915-933.
- Coveney, R.M., Jr., Murowchick, J.B., Grauch, R.I., Michael, D., Glascock, D., and Denison, J.D., 1992, Gold and platinum in shales with evidence against extraterrestrial sources of metals: *Chemical Geology*, v. 99, p. 101-114.
- Coveney, R.M., Jr., Grauch, R.I., and Murowchick, J.B., 1993, Ore mineralogy of nickel-molybdenum sulfide beds hosted by black shales of South China, in Reddy, R.G., and Weizenbach, R.N., eds., *The Paul E. Queneau Symposium—Extractive metallurgy of copper, nickel and cobalt*: Minerals, Metals and Materials Society, v. 1, p. 369-375.
- 1994, Metals, phosphate, and stone coal in the Proterozoic and Cambrian of China: The geological setting of precious metal-bearing Ni-Mo ore beds: *Society of Economic Geologists Newsletter*, no. 18, p. 1, 6-11.
- Crusius, J., and Thomson, J., 2000, Comparative behavior of authigenic Re, U, and Mo during reoxidation and subsequent long-term burial in marine sediments: *Geochimica et Cosmochimica Acta*, v. 64, p. 2233-2242.
- Du Andao, He Hongliao, and Yin Ningwan, 1995, A study of the rhenium-osmium geochronometry of molybdenites: *Acta Geologica Sinica*, v. 8, p. 171-181.
- Du Andao, Wang Shuxian, Sun Dezhong, Zhao Dunmin, and Liu Dunyi, 2001, Precise Re-Os dating of molybdenite using Carius tube, NTIMS and ICPMS: SGA-SEG Joint Biennial Meeting, Krakow, Poland, August 26-29, 2001, Proceedings, p. 405-407.
- Esser, B.K., and Turekian, K.K., 1993, The osmium isotopic composition of the continental crust: *Geochimica et Cosmochimica Acta*, v. 57, p. 3093-3104.
- Emerson, S.R., and Huested, S.S., 1991, Oceanic anoxia and the concentration of molybdenum and vanadium in seawater: *Marine Chemistry*, v. 34, p. 177-196.
- Fan Delian, Yang Xiuzhen, Wang Yufang, and Chen Nansheng, 1973, Petrological and geochemical characteristics of a nickel-molybdenum-multiple-element-bearing Lower Cambrian black shale from a certain district in south China: *Geochimica*, v. 3, p. 143-163.
- Fan Delian, Yang Ruiying, and Huang Zhongxiang, 1984, The Lower Cambrian black shales series and the iridium anomaly in south China: Developments in Geoscience, International Geological Congress, 27th, Moscow, 1984, Beijing, Science Press, p. 215-224.
- Fan Delian, Ye Jie, and Liu Tiebing, 1992, Black shale series-hosted silver-vanadium deposits of the Upper Sinian Duoshantuo Formation, western Hubei Province, China: *Exploration and Mining Geology*, v. 1, p. 29-38.
- Froelich, P.N., Klinkhammer, G.P., Bender, M.L., Luedtke, N.A., Heath, G.R., Culle, D., Dauphin, P., Hammond, D., Hatrman, B., and Maynard, V., 1979, Early oxidation of organic matter in pelagic sediments of the eastern equatorial Atlantic: Suboxic diagenesis: *Geochimica et Cosmochimica Acta*, v. 43, p. 1075-1090.
- Hannah, J.L., Scherstén, A., and Stein, H.J., 2001, Re-Os behavior in mafic magmas and terrestrial diagenetic materials: Extracting information from open systems: Geological Society of America, Abstracts with Programs, v. 33, no. 6, p. A-238.
- Hein, J.R., Fan Delian, Ye Jie, Liu Tiebing, and Yeh Hsueh-Wen, 1999, Composition and origin of Early Cambrian Tiantaishan phosphorite-Mn carbonate ores, Shaanxi Province, China: *Ore Geology Reviews*, v. 15, p. 95-134.
- Helz, G.R., Miller, C.V., Charnock, J.M., Mosselmans, J.F.W., Patrick, R.A.D., Garner C.D., and Vaughan, D.J., 1996, Mechanism of molybdenum removal from the sea and its concentration in black shales: EXAFS evidence: *Geochimica et Cosmochimica Acta*, v. 60, p. 3631-3642.
- Holland, H.D., 1979, Metals in black shales—a reassessment: *ECONOMIC GEOLOGY*, v. 74, p. 1676-1680.
- Horan, M.F., Morgan, J.W., Grauch, R.I., Coveney, R.M., Jr., Murowchick, J.B., and Hulbert, L.J., 1994, Rhenium and osmium isotopes in black shales and Ni-Mo-PGE-rich sulfide layers, Yukon Territory, Canada, and Hunan and Guizhou Provinces, China: *Geochimica et Cosmochimica Acta*, v. 58, p. 257-265.
- Jacobs, L., Emerson, S., and Huested, S.S., 1987, Trace metal chemistry of the Cariaco trench: *Deep-Sea Research*, v. 34, p. 965-981.
- Kao, L.-S., Peacor, D.R., Coveney, R.M., Jr., Zhao, G., Dungey, K.E., Curtis, M.D., and Penner-Hahn, J.E., 2001, A C/MoS<sub>2</sub> mixed-layer phase (MoSc) occurring in metalliferous black shales from southern China, and new data on jordisite: *American Mineralogist*, v. 86, p. 852-861.
- Landing, E., Bowring, S.A., Davidek, K.L., Westrop, S.R., Geyer, G., and Heldmaier, W., 1998, Duration of the Early Cambrian: U-Pb ages of volcanic ashes from Avalon and Gondwana: *Canadian Journal of Earth Sciences*, v. 35, p. 329-338.
- Large, D., 1976, Sediment-hosted submarine exhalative lead-zinc deposits—a review of their geological characteristics and genesis, in Wolf, K.H., ed., *Strata-bound and stratiform ore deposits*: Amsterdam, Elsevier, v. 9, p. 469-507.
- Liu, W., Boni, M., and Bechstdt, T., 1997, A first approach to the MVT ore deposits in the Cambrian of Hunan (southern China), in Papunen, H., ed., *Mineral deposits: Research and exploration—where do they meet?*: Rotterdam, Balkema, p. 539-541.
- Lott, D.A., Coveney, R.M., Jr., Murowchick, J.B., and Grauch, R.I., 1999, Sedimentary exhalative nickel-molybdenum ores in south China: *ECONOMIC GEOLOGY*, v. 94, p. 1051-1066.

- Loukola-Ruskeeniemi, K., and Heino, T., 1996, Geochemistry and genesis of the black shale-hosted Ni-Cu-Zn deposit at Talvivaara, Finland: *ECONOMIC GEOLOGY*, v. 91, p. 80–110.
- Mao Jingwen, 1995, Tourmalinite from northern Guangxi, China: *Mineralium Deposita*, v. 34, p. 235–245.
- Markey, R., Stein, H., and Morgan, J., 1997, Highly precise Re-Os dating for molybdenite using alkaline fusion and NTIMS, in Papunen, H., ed., *Mineral deposits: Research and exploration—where do they meet?*: Rotterdam, Balkema, p. 957–960.
- 1998, Highly precise Re-Os dating for molybdenite using alkaline fusion and NTIMS: *Talanta*, v. 45, p. 935–946.
- Mercone, D., Thomson, J., Croudace, I.W., and Troelstra, S.R., 1999, A coupled natural immobilisation mechanism for mercury and selenium in deep-sea sediments: *Geochimica et Cosmochimica Acta*, v. 63, p. 1481–1488.
- Murrowhick, J.B., Coveney, R.M., Jr., Grauch, R.I., and Chen Nancheng, 1992, Ni-Mo ores of southern China: Biologic, tectonic, and sedimentary controls on their origin [abs.]: *International Geological Congress, 29th, Kyoto, Abstracts*, v. 3, p. 2997.
- Murrowhick, J.B., Coveney, R.M., Jr., and Grauch, R.I., 1994, Cyclic variations of sulfur isotopes in Cambrian stratabound Ni-Mo-(PGE-Au) ores of southern China: *Geochimica et Cosmochimica Acta*, v. 58, p. 1813–1823.
- Nozaki, Y., 1997, A fresh look at element distribution in the North Pacific: [http://earth.agu.org/eos\\_elec/97025e.htm](http://earth.agu.org/eos_elec/97025e.htm)
- Pasava, J., Hladikova, J., and Dobes, P., 1996, Origin of Proterozoic metal-rich black shales from the Bohemian Massif, Czech Republic: *ECONOMIC GEOLOGY*, v. 91, p. 63–79.
- Peacor, D.R., Coveney, R.M., Jr., and Zhao, G., 2000, Authigenic illite and organic matter: The principal hosts of vanadium in the Mecca Quarry Shale at Velpen, Indiana: *Clay and Clay Minerals*, v. 48, p. 311–316.
- Pegram, W.J., Krishnaswami, S., Ravizza, G.E., and Turekian, K.K., 1992, The record of seawater  $^{187}\text{Os}/^{186}\text{Os}$  variation through the Cenozoic: *Earth and Planetary Science Letters*, v. 113, p. 569–576.
- Peng, G., 1986, The origin of stratabound Pb-Zn deposits in Huayuan, Hunan: *Scientia Geologica Sinica*, v. 2, p. 177–186 (in Chinese).
- Piper, D.Z., 1994, Seawater as the source of minor elements in black shales, phosphorites and other sedimentary rocks: *Chemical Geology*, v. 114, p. 95–114.
- Qiu Y., Gao, S., McNaughton, N.J., Groves, D.I., and Ling, W., 2000, First evidence of >3.2 Ga continental crust in the Yangtze craton of south China and its implications for Archean crustal evolution and Phanerozoic tectonics: *Geology*, v. 28, p. 11–14.
- Ravizza, G., and Turekian, K.K., 1989, Application of the  $^{187}\text{Re}$ - $^{187}\text{Os}$  system to black shale geochronometry: *Geochimica et Cosmochimica Acta*, v. 53, p. 3257–3262.
- Ravizza, G., Turekian, K.K., and Hay, B.J., 1991, The geochemistry of rhenium and osmium in recent sediments from the Black Sea: *Geochimica et Cosmochimica Acta*, v. 55, p. 3741–3752.
- Sharma, M., Papanastassiou, D.A., and Wasserburg, G.J., 1997, The concentration and isotopic composition of osmium in the oceans: *Geochimica et Cosmochimica Acta*, v. 61, p. 3287–3299.
- Shen, J.J., Papanastassiou, D.A., and Wasserburg, G.J., 1996, Precise Re-Os determinations and systematics of iron meteorites: *Geochimica et Cosmochimica Acta*, v. 60, p. 2887–2900.
- Shirey, S.B., and Walker, R.J., 1995, Carius tube digestion for low-blank rhenium-osmium analysis: *Analytical Chemistry*, v. 67, p. 2136–2141.
- Singh, S.K., Trivedi, J.R., and Krishnaswami, S., 1999, Re-Os isotope systematics in black shales from the Lesser Himalaya: Their chronology and role in the  $^{187}\text{Os}/^{188}\text{Os}$  evolution of seawater: *Geochimica et Cosmochimica Acta*, v. 63, p. 2381–2392.
- Smoliar, M.I., Walker, R.J., and Morgan, J.W., 1996, Re-Os ages of group IIA, IIIA, IVA and VIB iron meteorites: *Science*, v. 271, p. 1099–1102.
- Stein, H.J., Markey, R.J., Morgan, J.W., Du, A., and Sun, Y., 1997, Highly precise and accurate Re-Os ages for molybdenite from the East Qinling molybdenum belt, Shaanxi Province, China: *ECONOMIC GEOLOGY*, v. 92, p. 827–835.
- Steiner, M., 2001, Die fazielle Entwicklung und Fossilverbreitung auf der Yangtze Plattform (Südchina) im Neoproterozoikum/frühesten Kambrium: *Freiberger Forschungshefte*, v. C492, p. 1–26.
- Steiner, M., and Erdtmann, B.D., 2001, The Sancha-Wangjiashan section, Hunan Province, China: Occurrence of syngenetic Fe-Ni-Mo ore layers near the base of the lowermost Cambrian Niutitang Formation: *Paleoworld (Hefei, China)*, v. 13, p. 125–131.
- Steiner, M., Wallis, E., Erdtmann, B.D., Zhao, Y.L., and Yang, R.D., 2001, Submarine-hydrothermal exhalative ore layers in black shales from south China and associated fossils—insights into a Lower Cambrian facies and bio-evolution: *Paleogeography, Paleoclimatology, Paleocology*, v. 169, p. 165–191.
- Thomson, J., Higgs, N.C., Croudace, I.W., Coley, S., and Hydes, D.J., 1993, Redox zonation at an oxic/post-oxic boundary in deep-sea sediments: *Geochimica et Cosmochimica Acta*, v. 57, p. 579–595.
- Vine, J.D., and Tourtelot, E.B., 1970, Geochemistry of black shale deposits—a summary report: *ECONOMIC GEOLOGY*, v. 65, p. 253–272.
- Wang Zhongcheng, and Li Guizhi, 1991, Baryte and witherite deposits in Lower Cambrian shales of south China: Stratigraphic distribution and geochemical characterization: *ECONOMIC GEOLOGY*, v. 86, p. 354–363.
- Zeng Mingguo, 1998, Geological characteristics of the Huangjiawan Mo-Ni deposit and its development in the future: *Guizhou Geology*, v. 15, p. 305–310 (in Chinese).
- Zhou, Z., Wang, R., Zhuang, R., and Lao, C., 1983, The genesis of Yutang lead-zinc deposit, Huayuan, Hunan Province: *Chengdu College of Geology Journal*, v. 3, p. 1–20.

